communications biology

Article

https://doi.org/10.1038/s42003-024-06709-1

Interleukin-33 promotes intrauterine adhesion formation in mice through the mitogen-activated protein kinase signaling pathway

Check for updates

Dan Liu[1,2,3], Liwei Yuan[1,2], Fengjuan Xu[2,4,5], Yulan Ma[1,2,5], Huixing Zhang[6], Yiran Jin[2], Meixia Chen[4], Zhining Zhang[7] & Sang Luo[2,3]

IL-33 belongs to the inflammatory factor family and is closely associated with the inflammatory response. However, its role in the development of intrauterine adhesions (IUAs) remains unclear. In this study, the role of IL-33 in the formation of IUAs after endometrial injury was identified via RNA sequencing after mouse endometrial organoids were transplanted into an IUA mouse model. Major pathological changes in the mouse uterus, consistent with the expression of fibrotic markers, such as TGF-β, were observed in response to treatment with IL-33. This finding may be attributed to activation of the phosphorylation of downstream MAPK signaling pathway components, which are activated by the release of IL-33 in macrophages. Our study provides a novel mechanism for elucidating IUA formation, suggesting a new therapeutic strategy for the prevention and clinical treatment of IUAs.

The endometrium, the mucus lining of the uterus, plays a crucial role in the reproductive lifespan of a woman, and its cyclic regulation is governed by the steroid hormones estrogen and progesterone. Intrauterine adhesions (IUAs) can arise from damage to the basal layer of the endometrium due to trauma or infection, leading to clinical symptoms such as reduced menstrual flow, amenorrhea, infertility, and recurrent miscarriage. These issues substantially impact female reproductive health[1]. IUAs pose a major reproductive challenge to women worldwide, and 19% of women were found to experience IUAs after abortion[2]. Unfortunately, the prevailing treatment methods still rely on artificial hormones or intrauterine contraceptive devices (IUDs), which do not promote the restoration of endometrial structure and function[3]. Research has revealed that the local microenvironment of the uterine cavity following trauma may influence the function of stem/progenitor cells under abnormal inflammation and immunity, hindering the functional repair of the endometrium and leading to scar formation. Consequently, the ability of the uterine cavity to support the growth of fertilized eggs is lost[4]. Investigating the interaction between the microenvironment of the uterine cavity and the proliferation and differentiation of stem cells is critical for both clinical strategies and basic research concerning IUAs, providing valuable insights into this challenging infertility issue.

Building on the foundation of stem cell therapy, researchers have shown that organoids are promising candidates for injury and regenerative applications. Organoids are clonal structures derived from the in vitro proliferation and differentiation of stem cells, and their structure and function are similar to those of living organs. Organoids serve as "seed cells" for tissue and organ reconstruction[5]. In a mouse IUA model, endometrial epithelial cell-derived organoids were evaluated and found to rebuild the structural integrity of the endometrial epithelium after injury and respond to ovarian hormones, leading to enduring endometrial functional repair[6]. On the basis of these findings, we hypothesize that organoids influence the microenvironment at the injury site in the uterine cavity and that the altered factors in this microenvironment may directly or indirectly regulate critical signaling pathways involved in maintaining stem cell stemness and self-renewal capacity, thereby alleviating IUAs. This research has major clinical implications for addressing this challenging issue of refractory infertility.

Through transcriptomic sequencing analysis, we identified a significantly altered factor, interleukin-33 (IL-33), in uterine cavity tissue following organoid treatment. Research has established that IL-33 is an inflammatory and profibrotic factor involved in tissue repair processes[7]. As a member of the IL-1 family, IL-33 delivers signals through the ST2 receptor,

[1]Department of Gynecology, General Hospital of Ningxia Medical University, Yinchuan, China. [2]Department of Beijing National Biochip Research Center Sub-Center in Ningxia, Institute of Medical Sciences, General Hospital of Ningxia Medical University, Yinchuan, Ningxia, China. [3]Key Laboratory of Ministry of Education for Fertility Preservation and Maintenance, Ningxia Medical University, Yinchuan, Ningxia, China. [4]Ningxia Medical University, Yinchuan, China. [5]Ningxia Key Laboratory of Stem Cell and Regenerative Medicine, Yinchuan, Ningxia, China. [6]The First Affiliated Hospital of Zhengzhou University, Zhengzhou, China. [7]Department of Gynecological Oncology Surgery of the General Hospital of Ningxia Medical University, Yinchuan, China. e-mail: 175919898@qq.com

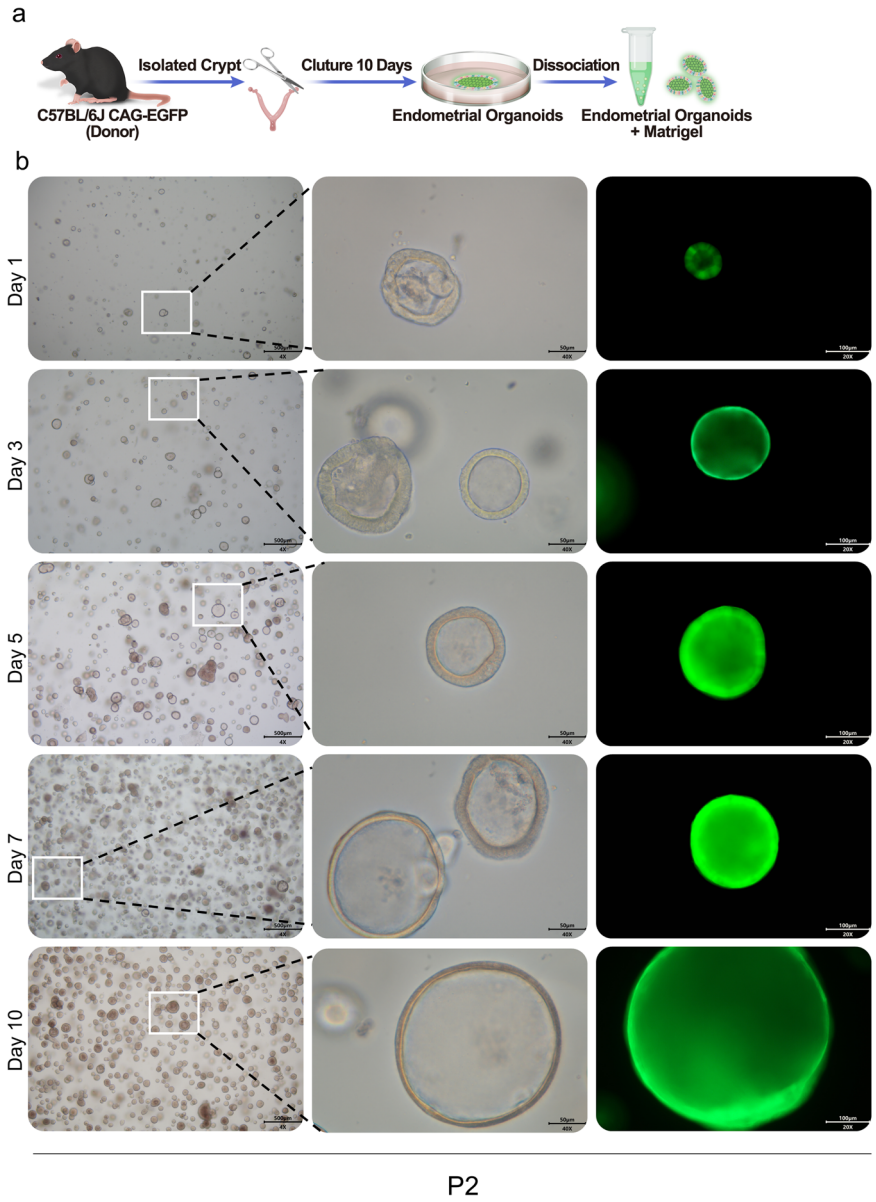

Fig. 1 | Cultivation and identification of mouse endometrial organoids. a Schematic diagram of female C57BL/6J mouse organoid culture. **b** Representative brightfield images of endometrial organoids at different time points were captured under a light microscope (×4, scale bar, 500 μm; ×40, scale bar, 50 μm; ×20, scale bar, 100 μm).

exerting proinflammatory and profibrotic functions[8]. IL-33 is known to be released during cell necrosis and is closely associated with tissue infection and trauma, resulting in its designation as an "alarm protein"[9,10]. Given these biological characteristics, IL-33 has attracted increased attention from researchers, leading to extensive studies exploring its role in immune regulation. Notably, IL-33 has been implicated in inflammation and pathological fibrosis, including its capacity to induce anaphylactic shock and contribute to fibrotic disease development[11,12]. In vivo, activation of the IL-33/ST2 signaling pathway is essential for the progression of severe liver fibrosis, cardiac fibrosis, and renal fibrosis[13]. Since its discovery in human tissues by Baekkevold et al. in 2003, IL-33 has been the subject of over 2000 studies to date[14]. As a "warning" cytokine, IL-33 is released in response to cellular damage, indicating tissue damage or inflammatory infection[15]. Despite the extensive study of the role of IL-33 in the immune system, its involvement in the formation of IUAs remains relatively unexplored.

Therefore, in this study, we not only induced the culture and transplantation of mouse endometrial organoids but also utilized transcriptomic sequencing to identify the changes in the uterine cavity microenvironment before and after organoid transplantation. This comprehensive approach aimed to elucidate the role of the inflammatory factor IL-33 in the formation of IUAs, with the hope of revealing the relationship between IL-33 and the development of IUAs. Ultimately, this research endeavors to provide novel treatment strategies for clinical applications.

Results

Culture of endometrium-derived organoids

In this study, we aimed to investigate the reparative potential of organoids on the endometrium. We isolated endometrium rich in epithelial cells from the mouse uterus and cultivated mouse endometrial organoids via our previously established culture method (Fig. 1a). After 10 days of culture, we observed a significant increase in the number of organoids. Furthermore, we observed that the volume of the organoids gradually increased with culture time, confirming the stable growth of the organoids in our established culture system (Fig. 1b).

RNA sequencing analysis of changes in the microenvironment of the uterine cavity in mice

To determine the impact of organoids on the microenvironment of the uterine cavity in mice with IUAs, we conducted transcriptomic sequencing to identify changes in genes and signaling pathways following orthotopic transplantation of endometrial organoids (Fig. 2a). Initially, we identified genes related to fibrosis in the NCBI database and performed cluster

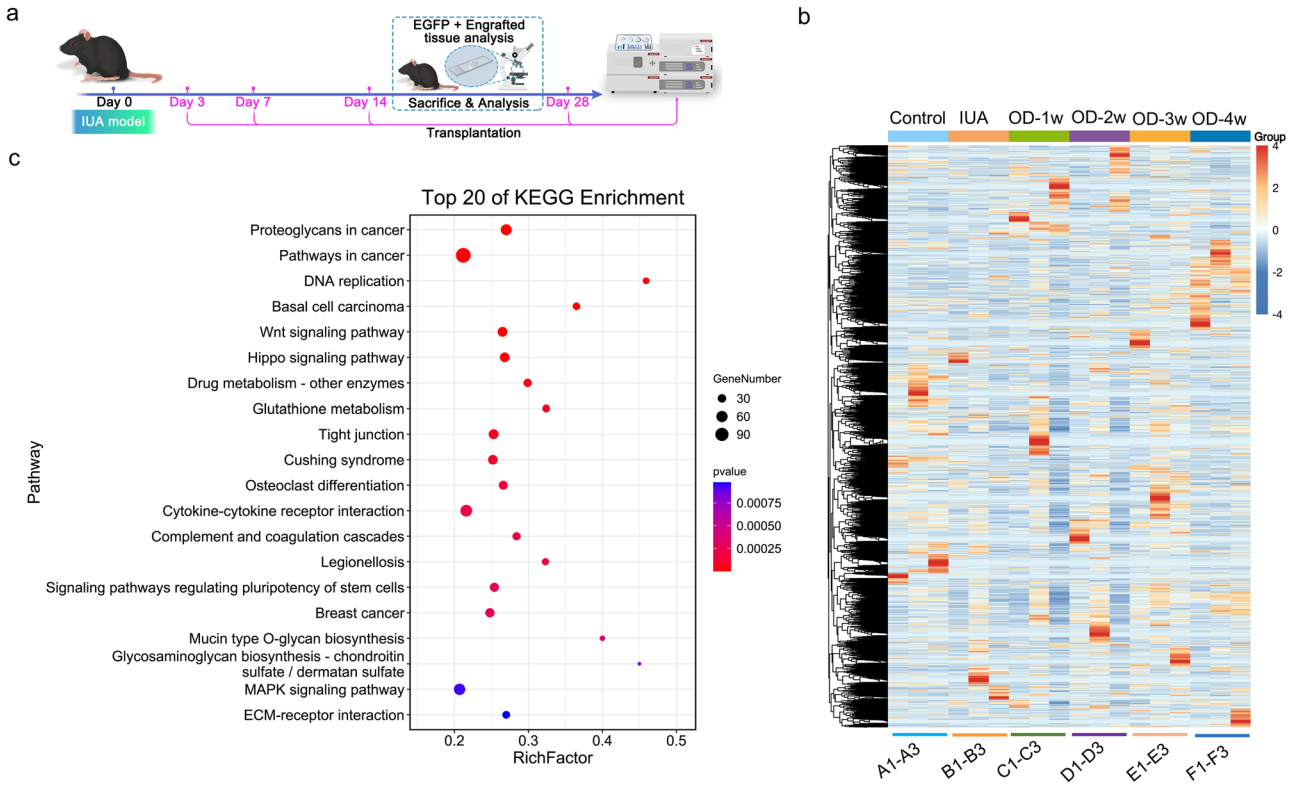

Fig. 2 | RNA sequencing (RNA-seq) analysis of changes in the microenvironment of the uterine cavity of mice. a Schematic diagram of the RNA-seq data of female C57BL/6 J mice. **b** Heatmap depicting all differentially expressed genes identified by RNA-seq analysis of the endometria from endometrial organoid-transplanted mice and normal mice. The colors range from blue (indicating low expression) to red (indicating high expression). OD organoid. **c** KEGG analysis of genes involved in the IL-33-related module (highlighted in blue). The size of the nodes represents the gene count, and the color of the nodes reflects the statistical significance represented as [−log10 (p value)]. The data are from one experiment with three biological replicates per group ($n = 3$).

heatmap analysis. This analysis revealed that IL-33 was highly expressed in the IUA model group and significantly decreased after transplantation. The heatmap highlighted two regular gene modules related to fibrosis: one module was highly expressed in the controls and expressed at low levels in all IUA models, whereas the other was expressed at low levels in the control group and the IUA model group; however, its expression was high in the first week after repair and decreased thereafter (Fig. 2b). Next, we conducted weighted correlation network analysis (WGCNA) using all the genes from all the samples, and we identified the gene module containing IL-33. We subsequently analyzed 440 genes within this module and found associations with the MAPK, Wnt, and Hippo signaling pathways. To explore the potential connection between IL-33 and the MAPK pathway, we selected models and organoids that exhibited significant changes after one week of repair and remained stable within the group for further analysis. We performed enrichment analysis via the ORA overcharacterized algorithm and generated a bubble diagram for the top 20 gene pathways (Fig. 2c). These results suggest a correlation between the MAPK signaling pathway and IL-33.

IL-33 expression was significantly increased in the IUA mouse model

The transcriptome sequencing results revealed a significant increase in the expression of IL-33 in the IUA mouse model, indicating a close association between IUAs and the inflammatory response. To further confirm the role of IL-33 in the formation of IUAs, we measured its expression level in the IUA model via enzyme-linked immunosorbent assays (ELISAs). Additionally, we investigated the ability of anti-IL-33 antibody (αIL-33) treatment to alleviate IUAs (Fig. 3a). After αIL-33 treatment for 3 days, the IL-33 level in the uterine cavity of the mice decreased significantly (Fig. 3b–d). Moreover, the expression levels of IL-1β, TNF-α, IL-6, and IL-10 were substantially lower than those in the IUA model group (Fig. 3e–i). This observation suggests that IL-33, which functions as a warning protein, is closely associated with the development of IUAs.

IL-33 significantly aggravated the pathological features of IUAs in the IUA mouse model

The main pathological changes observed in IUAs involve disordered regeneration of epithelial and mesenchymal cells at the endometrial base, excessive proliferation of fibroblasts, and abnormal accumulation of the extracellular matrix, all of which contribute to fibrous connective tissue hyperplasia and scar formation[16,17]. Abnormal fibroblast proliferation is considered a central mechanism in the pathogenesis of IUAs[18]. In our study, we observed changes in uterine morphology and analyzed the number of glands via hematoxylin–eosin (HE) staining (Fig. 4a, b). Additionally, we examined the extent of fibrosis through Masson staining (Fig. 4c). TGF-β, a well-known fibrosis-promoting factor, is an important marker for evaluating tissue fibrosis[19,20]. In the uterine cavity of the mice with IUAs treated with rmIL-33, we observed increased IUAs, reduced numbers of glands with fragmented and dissolved glands, thinning of the endometrium, substantial hyperplasia of fibrous tissue in the interstitium, and a notable increase in the expression of TGF-β (Fig. 4d). However, after αIL-33 treatment in the uterine cavity of the mice with IUAs, we observed a reduction in the fibrotic area and an increase in the number of glands. These results indicate that IL-33 aggravates the occurrence of IUAs and leads to more pronounced pathological features in mice with IUAs.

IL-33 inhibitors increased the expression level of endometrial stem cell markers

In female endometrial tissue, there are three main types of stem cells: epithelial stem cells, endothelial stem cells, and endometrial mesenchymal stem cells[21,22]. The renewal ability of these stem cells regulates the renewal and differentiation functions of the endometrium during the reproductive cycle. In our study, we evaluated changes in endometrial function by analyzing the

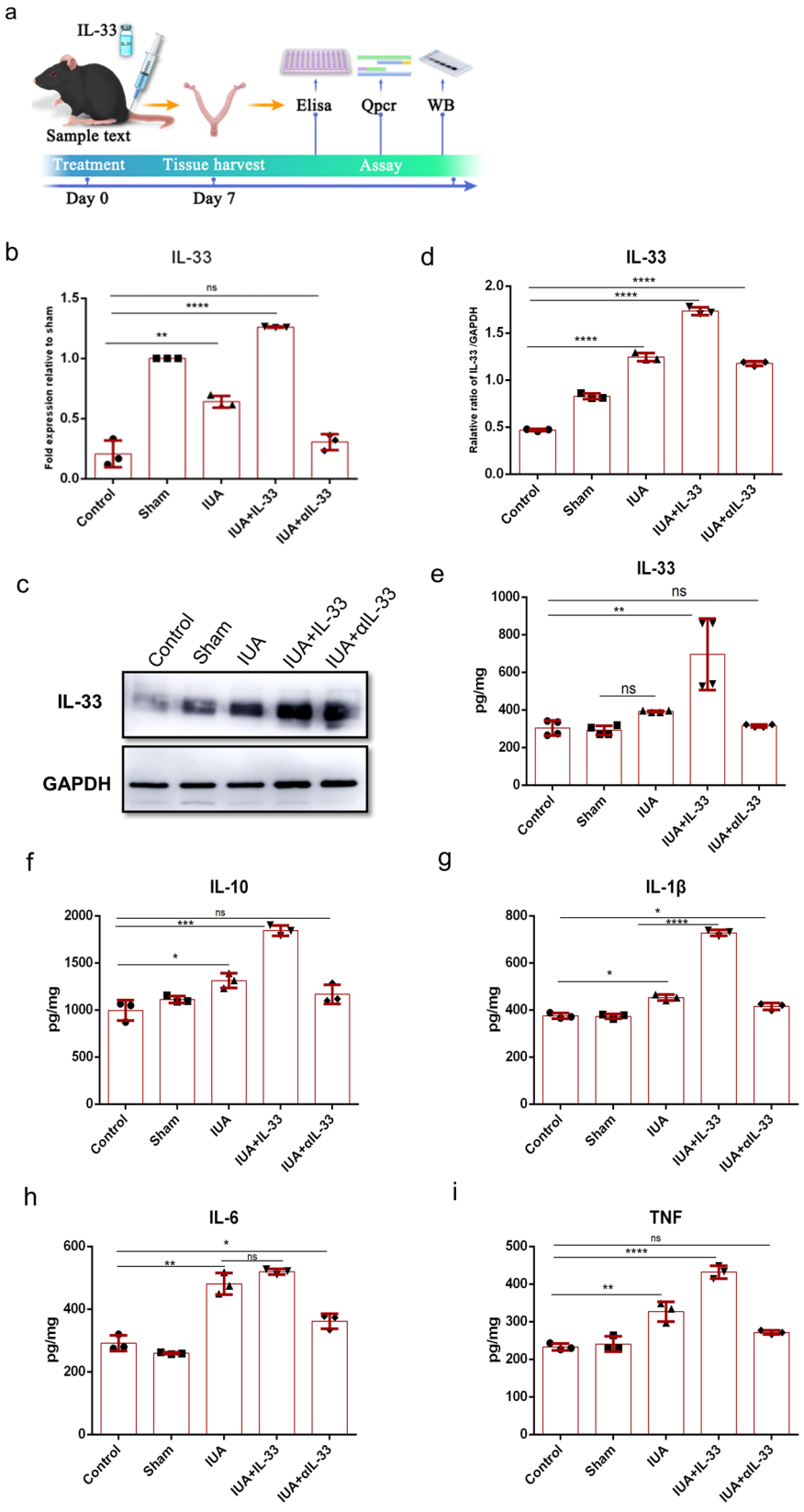

Fig. 3 | Expression level of IL-33 in the mouse uterus. a Schematic diagram of experiments carried out in mice. The mice were randomly assigned to the following groups (30 in each group): the control group; the sham operation group (sham), in which the mice underwent laparotomy without any treatment; the IUA model group (IUA), in which mice underwent induction of previously described mechanical damage; the rmIL-33-treated group (IUA + IL-33), in which mice experienced intrauterine injection of rmIL-33 (4 μg) on day 0 on both sides of the uterus during the mechanical scratching process; the αIL-33-treated group (IUA + αIL-33), in which the mice received an intrauterine injection of αIL-33 (10 μg) on both sides of the uterus on day 0 during the mechanical scratching process. The mice from each group were killed on day 7. **b**–**d** qPCR and Western blotting were employed to analyze the mRNA and protein levels of IL-33 in the endometrium. The full-length blots/gels are presented in Supplementary Fig. 2 (**e**–**i**). The protein levels of IL-33 and fibrogenic cytokines in the uterus were determined via ELISAs. The data are from one experiment with three independent experiments with three mice per group ($n = 3$). The values are the means ± SDs. $^{*}p < 0.05$, $^{**}p < 0.01$, $^{***}p < 0.001$, ns denotes $p > 0.05$ (unpaired Student's t test).

expression of stem cell renewal markers (FOXA2, SOX9, and SSEA1) and vascular endothelial markers (VEGF) (Fig. 5a). The results from Western blotting (Fig. 5b) and qRT-PCR (Fig. 5c) demonstrated that when the IUA mouse model was treated with αIL-33, the expression levels of endometrial stem cell renewal markers were significantly increased. However, there was no significant difference in the expression levels of stem cell renewal markers in the rmIL-33-induced group compared with those in the IUA model group.

Fertility evaluation

For determination of the degree of endometrial repair, fertility is a classic standard (Fig. 6a). In our study, we further investigated the role of IL-33 in the

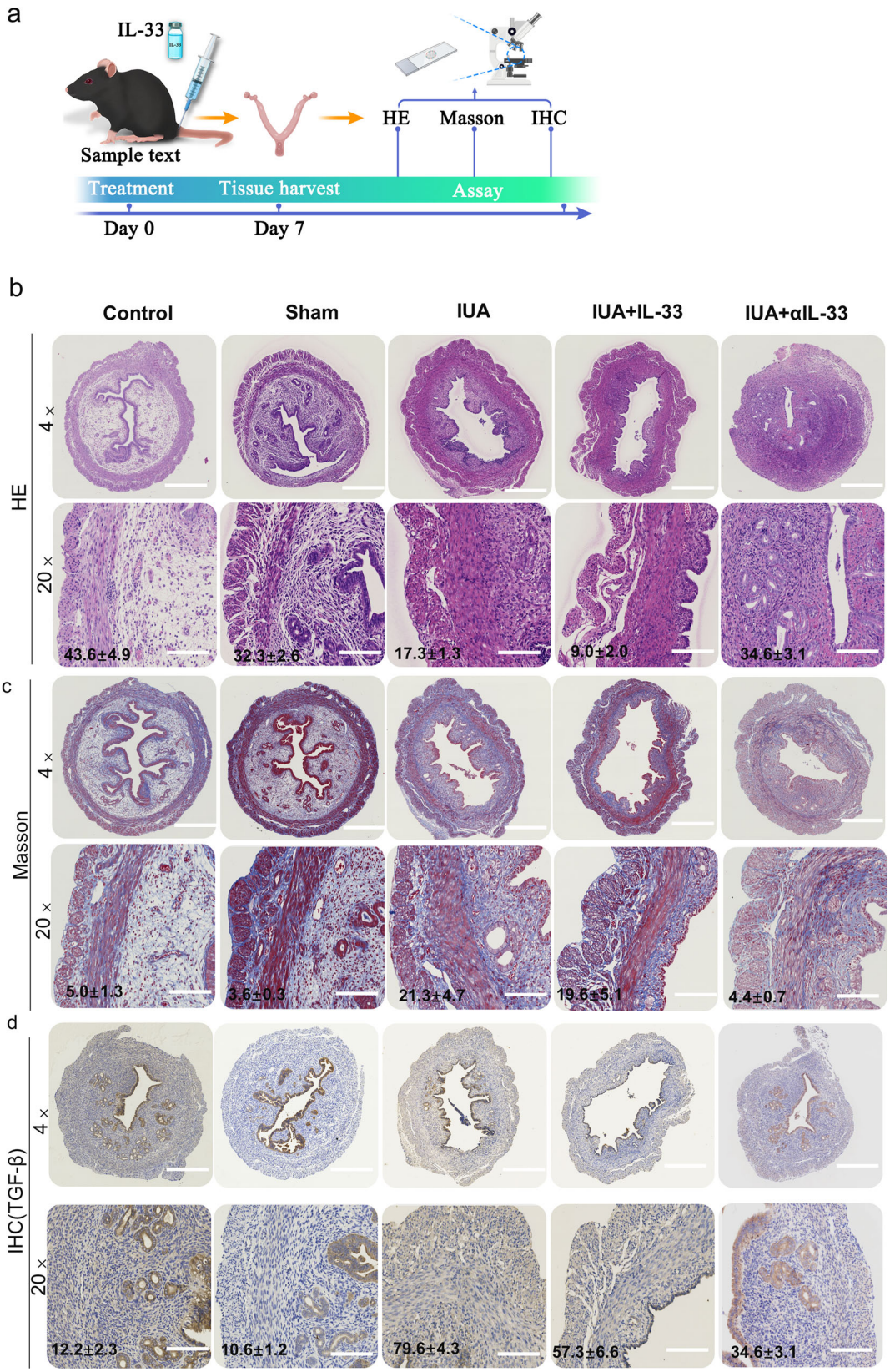

formation of IUAs by evaluating improvements in fertility in mice. During the mechanical scratching process, we injected 4 μg of rmIL-33 and 10 μg of αIL-33 into both sides of the uterus and mixed male and female mice in the cages on the 12th day after modeling. The day of vaginal plug detection was designated day 0 of gestation, and on day 30 of cocaging, the female mice were euthanized. The improvement in mouse fertility was assessed by observing the number of gestational sacs in mice from different pregnancy groups. The results revealed that the IUA model nearly completely lost fertility after rmIL-33 injury. However, the infusion of αIL-33 significantly rescued the fertility of the mice with IUAs, enabling them to conceive successfully (Fig. 6b, c).

Fig. 4 | Pathological features of IUAs in the IUA mouse model. a Schematic diagram of experiments carried out in mice. The mice were randomly assigned to the following groups (30 in each group): the control group; the sham operation group (sham), in which the mice underwent laparotomy without any treatment; the IUA model group (IUA), in which the mechanical damage of the mice was induced as previously described; the rmIL-33-treated group (IUA + IL-33), in which the mice received an intrauterine injection of rmIL-33 (4 μg) on both sides of the uterus on day 0 during the mechanical scratching process; and the αIL-33-treated group (IUA + αIL-33), in which the mice received an intrauterine injection of αIL-33 (10 μg) on both sides of the uterus on day 0 during the mechanical scratching process. The mice from each group were killed on day 7. **b** HE staining was performed to determine changes in the glands in each group at different stages of treatment. The capillaries of the IUA model group and the IUA+rmIL-33 group were disrupted and congested, and inflammatory cells infiltrated the stroma, as shown via HE staining. **c** Masson's trichrome staining was used to analyze changes in fibrosis in the different groups. **d** Immunohistochemical staining showing positive expression of TGF-β. The data are from one experiment with three independent experiments with three mice per group ($n = 3$) (×4, scale bar, 500 μm; ×20, scale bar, 100 μm). The results of the statistical analysis of the quantitative data are presented in Supplementary Fig. 1. The values are the means ± SDs. $^{*}p < 0.05$, $^{**}p < 0.01$, $^{***}p < 0.001$, ns denotes $p > 0.05$ (unpaired Student's t test).

IL-33 localization analysis and MAPK signaling pathway verification

To investigate the source of IL-33 production, we performed immunofluorescence (IF) staining to determine the correlation between IL-33 and macrophages. The results revealed that IL-33 and the macrophage marker F4/80 presented similar expression trends (Fig. 7). Therefore, we isolated monocytes/macrophages from mouse endometrial samples and determined IL-33 mRNA and protein expression in monocytes/macrophages. As shown in Supplementary Fig. 3, the expression of IL-33 was significantly greater in the IL-33-treated group than in the control group. After intervention with αIL-33, the expression of IL-33 decreased substantially. These findings suggest that macrophages are a major source of IL-33 production in the uterine cavity. Given that the inflammatory response is closely linked to the MAPK signaling pathway, we established a mouse organoid model to study the role of the downstream MAPK signaling pathway of IL-33 in the formation of IUAs (Fig. 8a, b). We analyzed key response targets of MAPK, including IL6, IL-1β, TGF-β, and α-SMA, at the mRNA expression level in endometrial organoids from each group. The results demonstrated that 3 μg of the ST2 inhibitor was optimal for alleviating the production of inflammatory factors (Fig. 8c). Next, we focused on the activation/phosphorylation levels of JNK, ERK, and P38 in endometrial organoids stimulated with 3 μg of ST2 inhibitor. The results showed that JNK, ERK, and P38 were inhibited by the ST2 inhibitor, similar to the effects observed with αIL-33 treatment. Conversely, the JUN/ERK/p38 signaling pathway was activated through rmIL-33, indicating that rmIL-33 can influence the expression levels of downstream molecules in the MAPK signaling pathway (Fig. 8d).

Discussion

The human endometrium exhibits a strong regenerative capacity, which is primarily attributed to the presence of endometrial stem/progenitor cells[23]. Tissue self-repair following uterine cavity trauma relies on the plasticity of differentiated cells and stem cells. These injuries lead to partial loss of resident stem cells. Additionally, abnormal inflammatory reactions in the microenvironment further impede the proper functioning of stem cells, ultimately resulting in a failure of functional regeneration[24]. Therefore, determination of the post-traumatic microenvironmental changes that affect stem cell proliferation and differentiation is crucial. This understanding is critical for guiding decisions regarding IUAs in clinical treatment, and these issues must be overcome before the clinical implementation of stem cell therapy.

In our study, we focused on comparing the microenvironment after organoids promoted endometrial repair, which revealed a significant and intriguing factor, IL-33. We further investigated the role of IL-33 in the development of IUAs.

IL-33 is a cytokine belonging to the IL-1 family that is abundantly expressed in endothelial cells, epithelial cells, and fibroblast-like cells, especially during inflammation. Upon tissue damage, IL-33 functions as an alarm signal, indicating tissue damage or inflammatory infection[25]. IL-33 can induce the expression of IL-4, IL-5, and IL-13, leading to severe pathological changes in injured organs. Studies by Lefrancais et al. demonstrated that in a mouse model of acute lung injury with alveolar epithelial damage and alveolar wall neutrophil accumulation, IL-33 levels significantly increased 2 h after injury and were involved in the development of pulmonary fibrosis[26]. However, the role of IL-33 in intrauterine trauma remains insufficiently explored. To elucidate the relationship between IL-33 and IUAs, we established an IUA mouse model through mechanical injury and introduced rmIL-33 and αIL-33 to assess their impact on injury and inflammation. The results indicated that the expression level of IL-33 was closely associated with the degree of adhesion in the mouse endometrium. To further examine the pathological changes induced by rmIL-33 in mouse endometrial adhesions, we analyzed alterations in the uterine gland and fibrotic areas via HE staining and Masson staining, respectively. We also precisely assessed the changes in the fibrosis index TGF-β through immunohistochemistry (IHC).

In subsequent investigations, we investigated the effects of rmIL-33 on the proliferation and self-renewal abilities of endometrial stem cells. We analyzed the expression levels of SOX9, Foxa2, and SSEA1 in the uterine cavity of the mice with IUAs via Western blotting. SOX9 is a marker gene for progenitor cells and is expressed in the basal endometrial glands in vivo, acting as a marker for stem cell renewal[27]. SSEA1 is a cell surface glycan expressed stage-specifically, with SSEA1+ cells located in epithelial and basal cells during the proliferative phase[28]. FoxA2 is critical for endometrial gland development and fertility in mice[29]. The results revealed that rmIL-33 significantly reduced the expression levels of epithelial stem cell markers and affected the expression of the vascular endothelial factor VEGF. Conversely, αIL-33 significantly normalized the proliferation of stem cells induced by mechanical damage and rmIL-33 stimulation.

Assessing fertility is the gold standard for evaluating the reproductive ability of mice. Consequently, we further evaluated the effect of αIL-33 on the fertility of mice with IUAs in vivo through male and female cage experiments. After 28 days of observation, αIL-33 significantly increased the formation of gestational sacs in the mice with IUAs. These findings further substantiate the importance of IL-33 in the pathological formation of IUAs following trauma and demonstrate the rescue effect of αIL-33 on this pathological process. These findings provide a new intervention strategy for the initial stage of IUA pathology.

As a cytokine with a "warning" function, IL-33 plays a critical role in innate immunity. Numerous cells can produce IL-33 in response to trauma, and our analysis of IUA tissue indicates that abnormal inflammatory responses play a role in the development of endometrial fibrosis. The potential relationship of macrophages, which are closely associated with inflammation, with IL-33 has garnered our interest. Consequently, we sought to trace the source of IL-33 and analyze its colocalization with macrophages through IF staining. The results revealed that the expression of IL-33 was the same as that of macrophages within the uterine cavity. To verify this result, we isolated macrophages from mouse uterine tissues via flow cytometry and analyzed the expression level of IL-33 in macrophages via qPCR and Western blotting. As expected, IL-33 expression was significantly increased in the IUA group and IUA + IL-33 group, whereas the expression level of IL-33 in macrophages was significantly decreased after αIL-33 treatment, which indicated that αIL-33 may reduce the release of IL-33 through macrophages, thus attenuating fibrotic development. These findings highlight macrophages as a major source of IL-33 production during endometrial injury and fibrosis in mice. The results suggest that IL-33 promotes endometrial fibrosis in a macrophage-dependent manner, providing a precise mechanism for

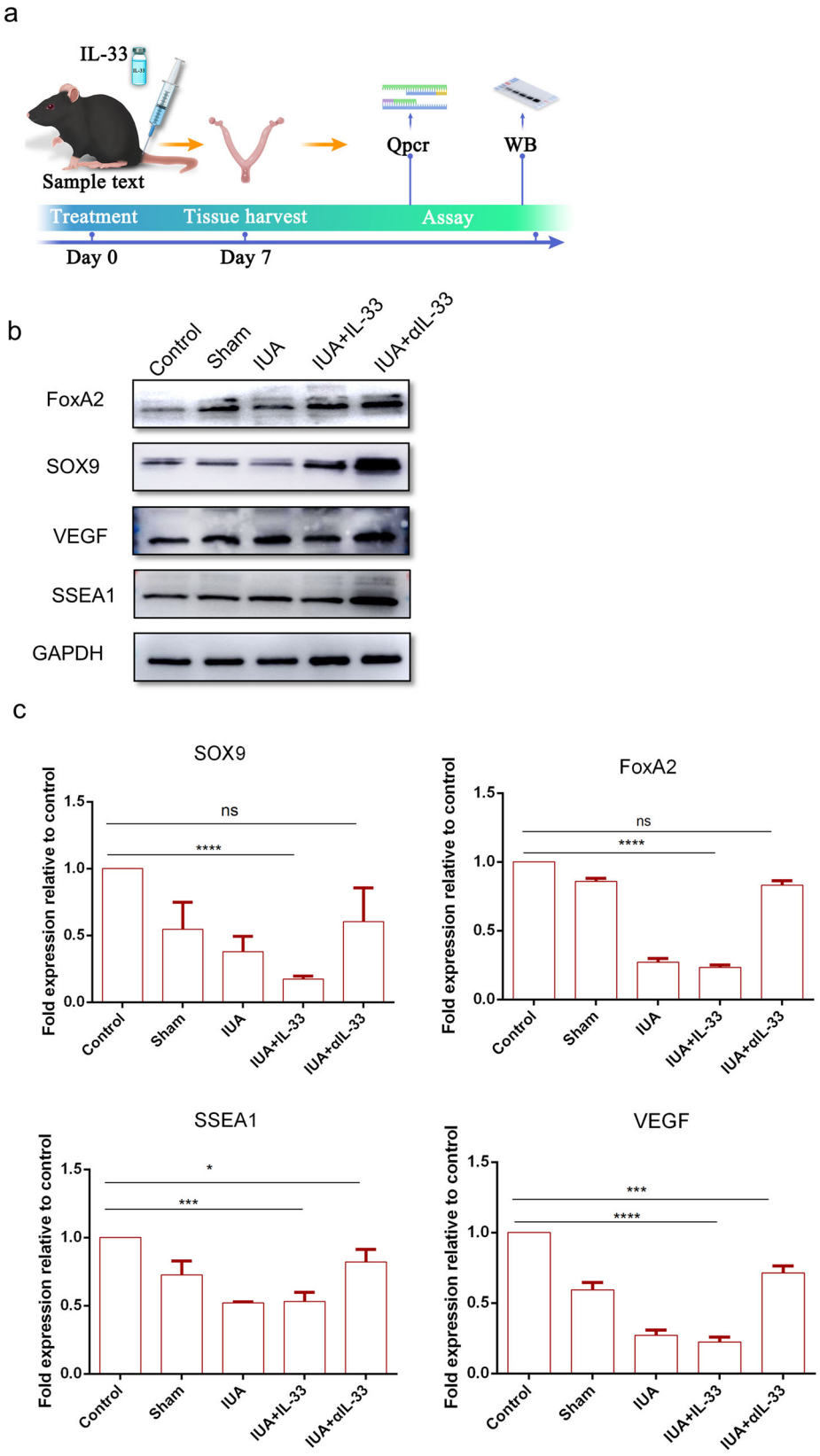

Fig. 5 | Increase in the expression of endometrial stem cell markers under αIL-33 treatment. **a** Schematic diagram of experiments carried out in mice. The mice were randomly assigned to the following groups (30 in each group): the control group; the sham operation group (sham), in which the mice underwent laparotomy without any treatment; the IUA model group (IUA), in which the mice underwent induction of previously described mechanical damage; the rmIL-33-treated group (IUA + IL-33), in which the mice experienced intrauterine injection of IL-33 (4 μg) on both sides of the uterus during the mechanical scratching process; and the αIL-33-treated group (IUA + αIL-33), in which the mice experienced intrauterine injection of αIL-33 (10 μg) on both sides of the uterus during the mechanical scratching process. The mice from each group were killed on day 7. **b** Western blotting was conducted to determine the protein levels of the stem cell markers in each group. The full-length blots/gels are presented, and statistical analysis of the quantitative results is presented in Supplementary Fig. 2. **c** qRT-PCR was used to measure the mRNA expression levels of SOX9, SSEA1, VEGF, and FoxA2 in the endometrial tissues of each group. The data are from one experiment with three independent experiments with three mice per group ($n = 3$). The values are the means ± SDs. $^{*}p < 0.05$, $^{**}p < 0.01$, $^{***}p < 0.001$, ns denotes $p > 0.05$ (unpaired Student's t test).

further exploration of the involvement of IL-33 in the pathogenesis of endometrial fibrosis.

When the body undergoes a stress response, a substantial amount of IL-33 is released, exerting its biological effects by binding to the specific receptor ST2[8]. Studies by Li et al.[30] demonstrated that IL-33 promotes the initiation and progression of pulmonary fibrosis by recruiting inflammatory cells and inducing their functions, leading to the production of fibrotic cytokines in an ST2- and macrophage-dependent manner. Given the presence of ST2 receptors on the cell membrane of macrophages, IL-33 may act on macrophages through the IL-33/ST2 signaling axis, thereby promoting macrophage polarization and participating in the pathological development of endometrial fibrosis.

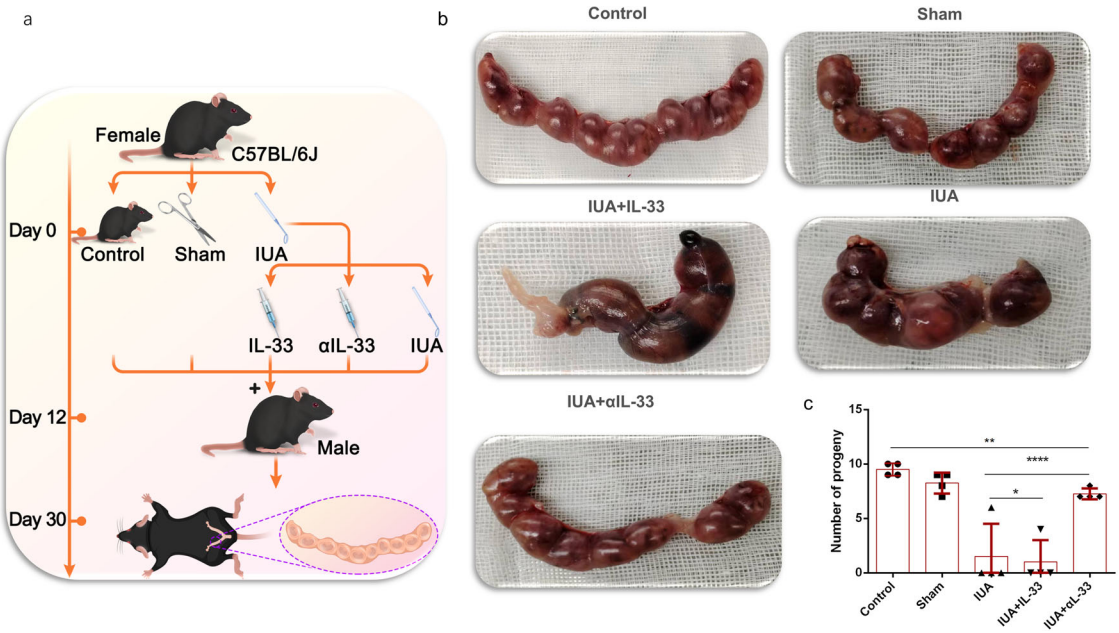

Fig. 6 | The pregnancy rate changed after treatment with αIL-33. a Schematic diagram of the experiments carried out in mice. **b** Representative images of embryos in the uterine cavity in each group. **c** Quantitative analysis of the pregnancy rate in each group. The data are from three independent experiments with three mice per group ($n = 3$). The values are the means ± SDs. $^{*}p < 0.05$, $^{**}p < 0.01$, $^{***}p < 0.001$, ns denotes $p > 0.05$ (unpaired Student's t test).

Typically, the IL-33/ST2/IL1RAcP complex initiates signaling through kinases, such as the MyD88 adapter, ultimately activating the MAP kinase pathway[8,31]. The MAPK signaling pathway plays a pivotal role in regulating the occurrence and development of inflammation. In a study by Tang et al., after 14 days of oral administration of gentamicin in rats, the expression levels of ERK1/2, JNK1/2, and p38 in kidney tissue significantly increased[32]. To determine whether the IL-33/ST2 signaling pathway also activates MAPK family-related signaling molecules during the development of IUAs, we examined the changes in endometrial signaling pathways induced by rmIL-33 through western blotting. We observed that the expression levels of ERK1/2, JNK1/2, and p38 were significantly greater in the rmIL-33 group than in the αIL-33 rescue group, whereas the phosphorylation levels of the corresponding signaling molecules were significantly lower in the rmIL-33 group than in the αIL-33 rescue group. These findings indicate that IL-33 released by cells binds to the ST2-specific receptor on the macrophage membrane and participates in the pathological formation of IUAs by altering the phosphorylation of the MAPK signaling pathway.

Although we have successfully revealed the role of IL-33 in the development of IUAs and explored its regulatory mechanism, the relationship between IL-33 and macrophages remains unclear, and further research is needed to understand how this molecule regulates macrophage function. Specifically, whether the polarization of M1 and M2 macrophages is related to the expression of IL-33 requires further investigation.

Methods

Animals

Female C57BL/6 J mice aged 6–8 weeks and weighing 18–20 g were procured from the experimental animal center of Ningxia Medical University. All the experimental procedures were conducted with the approval of the Ethics Committee of the General Hospital of Ningxia Medical University (Ethics Approval No. KYLL-2022-0460). We have complied with all relevant ethical regulations for animal use.

Inclusion and exclusion criteria

The animals were included in the study if they successfully experienced mechanical damage, which was defined by capillaries breaking and forming congestion and inflammatory cells infiltrating the stroma, as determined through HE staining. The animals were excluded if they died prematurely, preventing the collection of behavioral and histological data.

Blinding/masking

For each animal, three different researchers participated as follows: the first investigator was responsible for the anesthetic procedure. The second investigator administered the treatment according to the randomization table. Finally, a third investigator performed the surgical procedure.

Animal model of IUAs and treatment

Female C57BL/6 J mice were subjected to mechanical damage to establish the IUA model. Briefly, under sterile conditions, the mice were anesthetized with 5% pentobarbital sodium (5 mg/kg) before the abdominal cavity was opened to expose the uterine horn. A 5 mm uterine curette was then used to gently scrape both sides of the uterus until the uterine wall became pale and rough. The wound was disinfected with iodophor solution and sutured via 5-O lines.

In this study, the mice were randomly assigned to various groups (30 in each group), including the control group. In the sham operation group (sham), the mice underwent laparotomy without any treatment. In the IUA model group (IUA), the mechanical damage of the mice was induced as previously described. In the rmIL-33-treated group (IUA +rmIL-33), the mice received an intrauterine injection of rmIL-33 on both sides of the uterus on day 0 during the mechanical scratching process. In the αIL-33-treated group (IUA + αIL-33), the mice received an intrauterine injection of αIL-33 on both sides of the uterus on day 0 during the mechanical scratching process. The mice from each group were killed on day 7.

Establishment and transplantation of mouse endometrial organoids

After the mouse was killed, the uterus was removed from the opened abdominal cavity and washed with PBS before being dissected into small fragments. The fragments were digested at 37 °C for 50 min with 0.4 mg/ml collagenase V (Sigma) and 1.25 U/ml Dispase II while gently shaking. The digestion reaction was neutralized by adding 10 ml of DMEM/F12 containing 1% antibiotic. The mixed solution was washed three times with PBS,

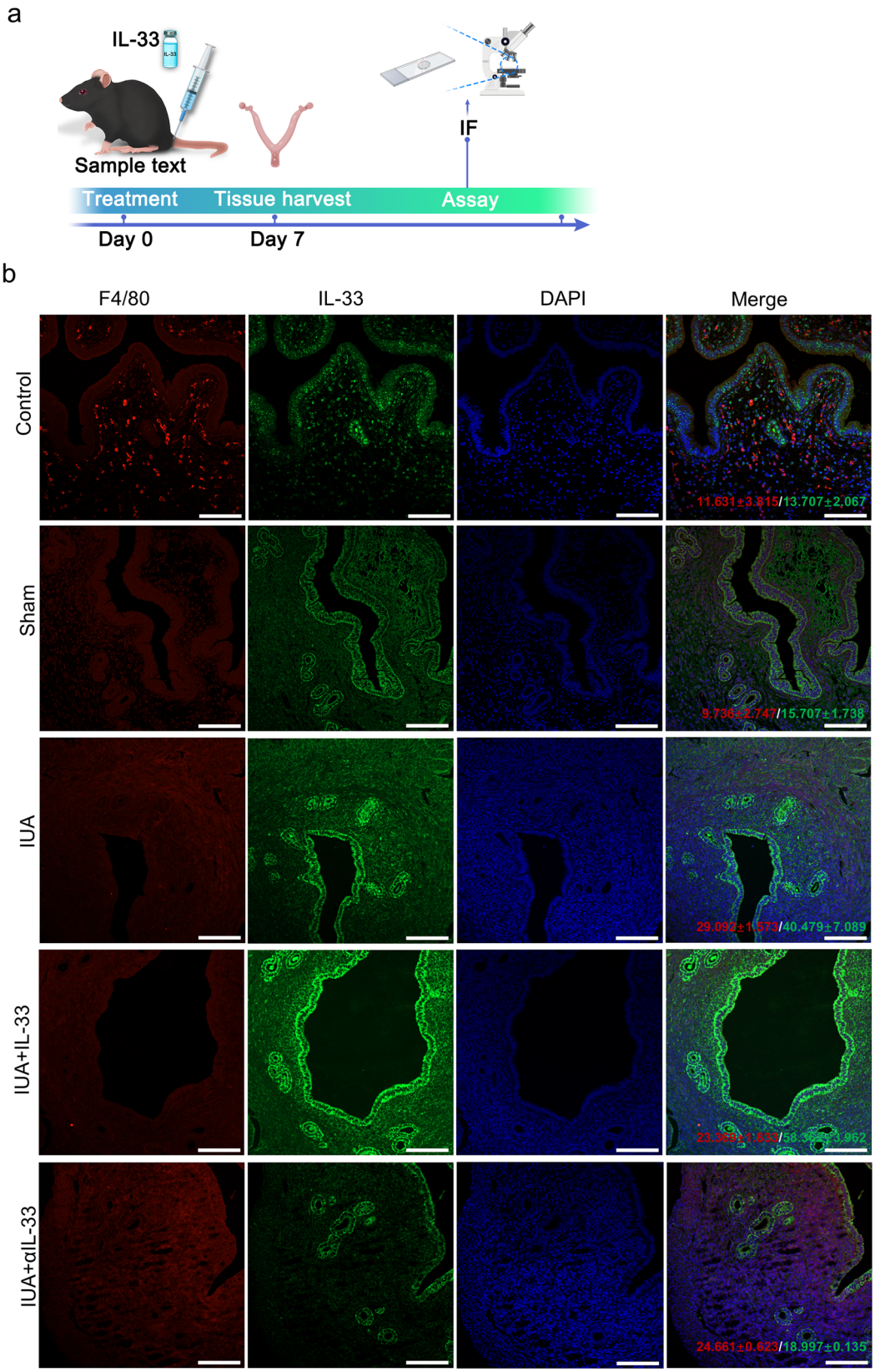

Fig. 7 | Macrophages are the source of IL-33 production. a Schematic diagram of experiments in the mouse uterus. **b** IF staining to determine the protein levels of IL-33 and F4/80 in endometrial tissues (×40, scale bar, 50 μm). The data are from one experiment with three independent experiments with three mice per group ($n = 3$). The values are the means ± SDs. $^{*}p < 0.05$, $^{**}p < 0.01$, $^{***}p < 0.001$, ns denotes $p > 0.05$ (unpaired Student's t test).

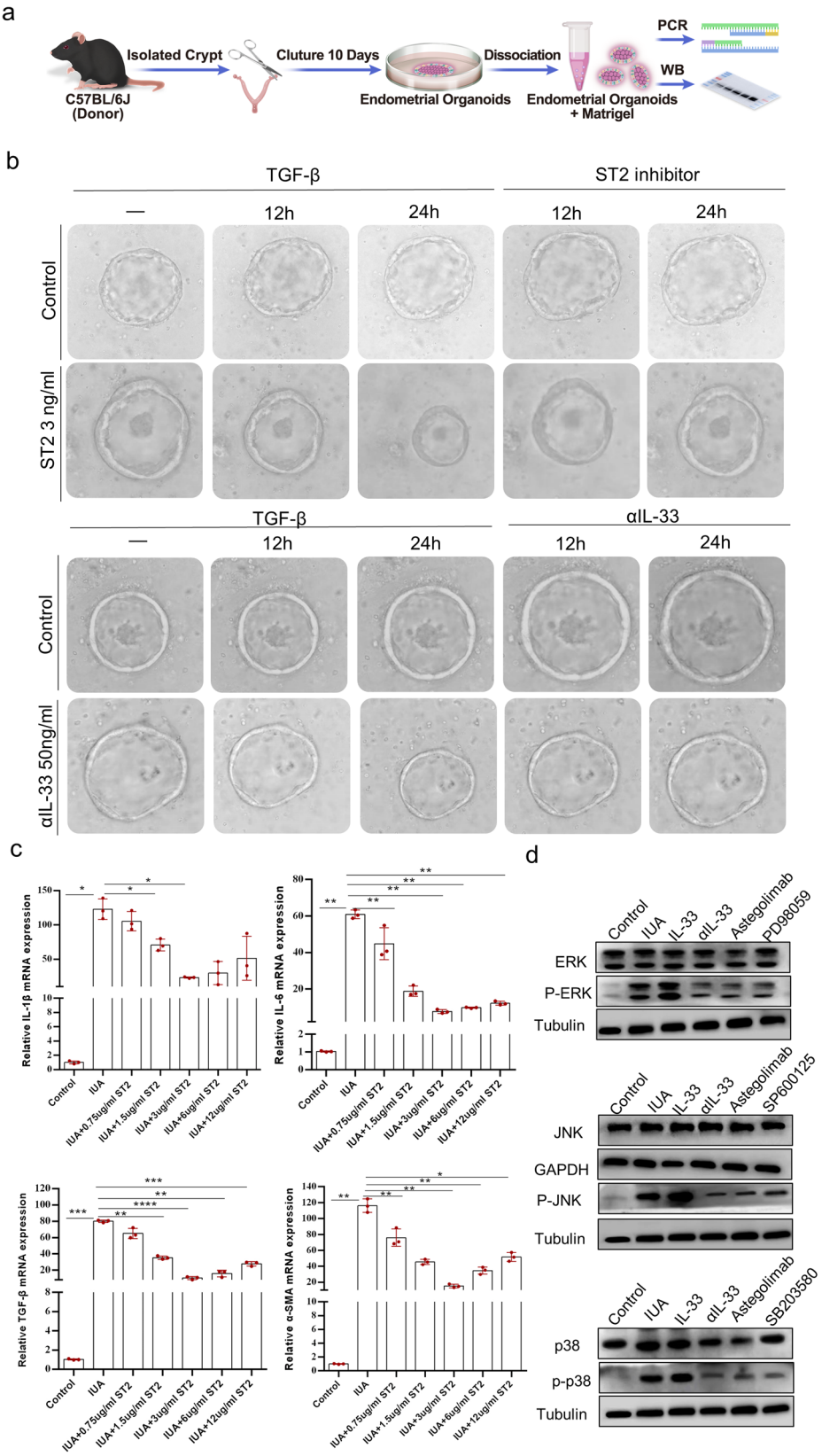

Fig. 8 | IL-33 activates the formation of IUAs via the MAPK signaling pathway. a Schematic diagram of mouse organoid culture and experiments carried out in mice. **b** Representative images of endometrial organoids treated with ST2 inhibitors at different time points were captured under a light microscope. The results of the gradient concentration experiment for ST2 are presented in Supplementary Fig. 4. **c** qRT-PCR analysis of the mRNA expression levels of *IL6*, *IL-1β*, *TGF-β*, and *α-SMA* in endometrial organoids. **d** The protein expression levels of JNK, ERK, and p38 were measured via Western blotting after endometrial organoids were treated with the JNK inhibitor SP600125, the ERK/MEK1 inhibitor PD98059, or the p38 inhibitor SB203580 before rmIL-33 was added at 100 ng/ml. Full-length blots/gels are presented, and the results of the statistical analysis of the quantitative results are presented in Supplementary Fig. 5. The data are from one experiment with three independent experiments with three mice per group ($n = 3$). The values are the means ± SDs. $^{*}p < 0.05$, $^{**}p < 0.01$, $^{***}p < 0.001$, ns denotes $p > 0.05$ (unpaired Student's t test).

and the flowthrough solution was collected after passing through a 100 μm cell filter and centrifuged at 1200 × g for 5 min. The pellet was resuspended in Matrigel (Corning) at a volume ratio of 1:1.5, and 20 μl of the Matrigel-cell mixture was transferred into each well of a 24-well plate and cultured in medium containing the following components: 500 ng/ml R-spondin 1, 80 ng/ml EGF, 150 ng/ml Noggin, 150 ng/ml Wnt3a, 1.25 mM *N*-acetylcysteine, 5 ng/ml FGF-10, 30 ng/ml KIAA1199, B27 (1X), 100 nM CHIR99021, 8 μM A83-01, 8 μM RKI-1477, 10 mM nicotinamide, 50 ng/ml HGF, N2 (1X), and 100 μg/ml primary cell antibiotic. The cells were cultured at 37 °C, 5% CO_2, and saturated humidity. The culture medium was changed every 2 days, and the organoids were passaged every 7–10 days at a 1:2 passage ratio.

Table 1 | Primers used for real-time quantitative PCR

Gene	Sequence (5′ → 3′)
SOX9 (F)	CACTACAGCGAGCAGCAGCAG
SOX9 (R)	GGGTGATGGGCGGGTAGGAG
FOXA2 (F)	CTGAAGCCCGAGCACCATTACG
FOXA2 (R)	GGTGGTGGCTGTGGTGATGTTG
SSEA-1 (F)	GCCCAGATCGTGCCAACTATGAG
SSEA-1 (R)	GCAGCCAGGGAAGCAGCATTAG
VEGF (F)	TGAACTTTCTGCTCTCTTG
VEGF (R)	TCGGGGTACTCCTGGAAGA
IL-33 (F)	CAAAGTTCAGCAGCACCGC
IL-33 (R)	T GTGTCAACAGACGCAGCAAA
GAPDH (F)	C CTCGTCCCGTAGACAAAATG
GAPDH (R)	T GAGGTCAATGAAGGGGTCGT

Table 2 | Antibodies used for immunofluorescence and western blotting

Marker (species)	Application (dilution)	Distributor (catalog number)
Primary antibodies		
SOX9 (Mouse)	WB (1:5000)	Proteintech (67439-1-Ig)
SSEA1 (Rabbit)	WB (1:1000)	ABclonal (A16320)
FOXA2 (Rabbit)	WB (1:1000)	Proteintech (22474-1-AP)
VEGF (Rabbit)	WB (1:1000)	Proteintech (19003-1-AP)
IL-33 (Mouse)	WB (1:1000)	Proteintech (66235-1-Ig)
IL-33 (Rabbit)	IF (1:500)	Servicebio (GB145309)
F4/80 (Rat)	IF (1:1000)	Servicebio (GB113373)
TGF-β (Rabbit)	IHC (1:500)	Servicebio (GB11179)
GAPDH (Rabbit)	WB (1:5000)	Proteintech (10494-1-AP)
Secondary antibodies		
Goat anti-rabbit IgG-HRP (H+L)	WB (1:1000)	ABclonal (AS028)
Goat anti-mouse IgG-HRP	WB (1:10,000)	ABclonal (AS066)
Goat anti-mouse IgG-FITC	IF (1:200)	Servicebio (GB22302)
Goat anti-mouse IgG-Cy3	IF (1:300)	Servicebio (GB21303)
Goat anti-rabbit IgG-HRP	IHC (1:200)	Servicebio (GB23303)

After 7 days of establishment of the IUA model, the abdominal cavities of the mice were opened under sterile conditions to expose the uterine horns. Then, 40 μl of 1×10^7 mature organoids were transferred into each uterine cavity. Finally, the uterus and abdominal cavity were cleaned, and the wound was sutured after disinfection with iodophor solution.

RNA sequencing

Total RNA was extracted from the organoids via an mRNA isolation kit following the manufacturer's protocol. The integrity of the RNA was assessed via an Agilent 2100 Bioanalyzer, and samples with an RNA integrity number (RIN) ≥7.5 were selected for further analysis. Libraries were constructed using TruSeq stranded total RNA with Ribo-zero Gold according to the manufacturer's instructions. These libraries were then sequenced on the Illumina sequencing platform, generating 150 bp/125 paired-end reads. Differentially expressed genes were used to generate heatmaps, and pathway analysis was performed via the KEGG pathway database.

HE staining and Masson's trichrome staining

At the end of each treatment, the rat uterine tissues were fixed in 4% paraformaldehyde for 24 h and subsequently processed for paraffin embedding. The paraffin-embedded sections were sliced into 4-μm sections and stained with HE and Masson's trichrome using standard protocols provided by Servicebio (Cat No. G1003; G1006). The images of the Masson-stained tissues were analyzed via ImageJ software to calculate the area of fibrosis, and the number of endometrial glands with H&E staining was counted in the horizontal sections.

Analysis of IL-33 by ELISAs

The weight of the animal tissue was accurately weighed, and 9 volumes of homogenization medium (0.9% saline) were added at a ratio of weight (mg):volume (μl) = 1:9. The homogenate was mechanically homogenized in an ice–water bath, prepared as a 10% homogenate, and centrifuged for 10 min at 3000 rpm, after which the supernatant was collected for the assay. The levels of IL-33, IL-1β, TNF-α, IL-6, and IL-10 in the serum from the IUA- and rmIL-33-treated models were determined via ELISAs via kits from Proteintech (Cat No. KE10054, Cat No. KE10003, Cat No. KE10002, Cat No. KE10007, Cat No. KE10008) according to the manufacturer's instructions.

Gene expression analysis by real-time PCR

Total RNA was extracted from the mouse uterus via the MiniBEST Universal RNA Extraction Kit (TaKaRa, Cat No. 9767) following the manufacturer's instructions. The PrimeScript™ RT reagent kit, gDNA Eraser (Perfect Real Time) (TaKaRa, Cat No. rr047), was used to synthesize cDNA, which was then subjected to amplification via real-time fluorescence PCR. RT–PCR analysis was conducted via the ABI Prism 7500 Sequence Detection System from Applied Biosystems. The sham operation group served as the control group, and its value was considered 1. The fold change in the mRNA levels was determined via the $2^{-\Delta\Delta Ct}$ method. Details of all the primers used for real-time quantitative PCR are provided in Table 1.

Western blotting for analysis of protein expression in uterine tissues

The tissue block was washed 3 times with precooled PBS to remove blood contamination, cut into small pieces and placed in a homogenizing tube. Two 4 mm homogenizing beads were added, 10 times the volume of tissue lysate (RIPA, Leagene, Cat No. PS0033) was added, and the homogenization program was set to homogenization. The homogenized tubes were removed, and the lysate was placed on ice for 30 min. The mixture was shaken every 5 min to ensure complete tissue lysis. The mixture was centrifuged at 12,000 rpm and 4 °C for 10 min, and the supernatant was collected as the total protein mixture. The protein concentration was measured via a BCA protein assay kit (KeyGEN, Cat No. KGP903). Proteins were resolved by 10% SDS-PAGE and then transferred to nitrocellulose membranes (EMS Millipore). The membranes were blocked with 5% skim fat milk containing 0.1% Tween 20 for 1 h at room temperature. The membranes were subsequently incubated with the relevant primary antibodies at 4 °C overnight. After being washed three times in TBS-T, the membranes were incubated with the secondary antibody for another hour at 37 °C. The target proteins were visualized via enhanced chemiluminescence (ECL) with a BioImaging System (Bio-Rad). Mouse monoclonal anti-GAPDH was used as a control for protein loading. Details of all the antibodies used are listed in Table 2.

Immunohistochemistry

Uterine tissue samples were fixed in 4% paraformaldehyde and embedded in paraffin. After antigen retrieval to activate endogenous peroxidase, the sections were incubated in 3% hydrogen peroxide for 30 min. The samples were then blocked with 10% normal goat serum for 1 h. The expression of TGF-beta was determined by incubating the sections with the primary antibody at 4 °C overnight. The slides were subsequently incubated with the secondary antibody dilution and then treated with DAB solution for 1 h.

Hematoxylin solution was briefly applied for 15 seconds to stain the nuclei. Finally, the slides were examined under a microscope. Details of the antibodies used are listed in Table 2.

Immunofluorescence

Uterine tissues were fixed with 4% paraformaldehyde, permeabilized with 0.5% Triton X-100 for 20 min at 37 °C, and blocked with 1% bovine serum albumin (BSA). The tissues were then stained with appropriate primary antibodies (Table 1) overnight at 4 °C. Subsequently, relevant fluorescent-conjugated secondary antibodies were used at appropriate concentrations, followed by nuclear staining with 4′,6-diamidino-2-phenylindole (DAPI). Image acquisition and processing were performed via a fluorescence microscope. The positive cells were counted via IPP6.0 software. All the antibodies used are listed in Table 2.

Monocyte/macrophage isolation

The mouse endometrial samples were rinsed three times with PBS until there were no obvious blood clots, after which they were cut into small pieces. Endometrial cells from five mice in each group were obtained by digesting the uterine tissue with 5 ml of 0.1% IV collagenase I (Gibco) for 1.5 h at 37 °C and mechanical dissociation through a 100-μm cell strainer. After centrifugation at 1800 rpm for 5 min, the cells were resuspended in 5 ml of red blood cell lysis buffer (eBisosciences). Monocyte macrophages were then obtained via density gradient centrifugation with a 50:50% Percoll (Solarbio) gradient at 2000 rpm for 20 min.

Statistics and reproducibility

For all data analysis, we used GraphPad Prism 6.0 software, and the results are presented as the means ± standard deviations (SDs). To compare differences between two groups, we employed Student's *t* test. For multiple comparisons, one-way or two-way ANOVA was used, as appropriate. A P value less than 0.05 was considered statistically significant. Each experiment was repeated independently three times for each group.

Reporting summary

Further information on research design is available in the Nature Portfolio Reporting Summary linked to this article.

Data availability

All primary data generated or analyzed in this study are available on request from the authors. Source data behind the figures can be found in Supplementary Data sheet 1. Raw long-read RNA sequencing data generated and utilized in the present study are also publicly available in NIH Sequence Read Archive (SRA) (accession no. PRJNA1129676) https://www.ncbi.nlm.nih.gov/sra/PRJNA1129676. The other datasets generated and/or analyzed during the current study are available from the corresponding author on reasonable request.

Received: 5 November 2023; Accepted: 9 August 2024;
Published online: 20 August 2024

References

1. Yu, Y. et al. Clinical features of the predilection and severer sites of intrauterine adhesions. *Zhong Nan Da Xue Xue Bao Yi Xue Ban.* **47**, 1568–1574 (2022).
2. Hooker, A. B. et al. Systematic review and meta-analysis of intrauterine adhesions after miscarriage: prevalence, risk factors and long-term reproductive outcome. *Hum. Reprod.* **20**, 262–278 (2014).
3. Xin, L. et al. A collagen scaffold loaded with human umbilical cord-derived mesenchymal stem cells facilitates endometrial regeneration and restores fertility. *Acta Biomater.* **92**, 160–171 (2019).
4. Gürgan, T. et al. Systematic and standardized hysteroscopic endometrial injury for treatment of recurrent implantation failure. *Reprod. Biomed. Online* **39**, 477–483 (2019).
5. Kim, J., Koo, B. K. & Knoblich, J. A. Human organoids: model systems for human biology and medicine. *Nat. Rev. Mol. Cell Biol.* **21**, 571–584 (2020).
6. Zhang, H. et al. Organoid transplantation can improve reproductive prognosis by promoting endometrial repair in mice. *Int J. Biol. Sci.* **18**, 2627–2638 (2022).
7. Brocker, C., Thompson, D., Matsumoto, A., Nebert, D. W. & Vasiliou, V. Evolutionary divergence and functions of the human interleukin (IL) gene family. *Hum. Genomics* **5**, 30–55 (2010).
8. Schmitz, J. et al. IL-33, an interleukin-1-like cytokine that signals via the IL-1 receptor-related protein ST2 and induces T helper type 2-associated cytokines. *Immunity* **23**, 479–490 (2005).
9. Lamkanfi, M. & Dixit, V. M. IL-33 raises alarm. *Immunity* **31**, 5–7 (2009).
10. Moussion, C., Ortega, N. & Girard, J. P. The IL-1-like cytokine IL-33 is constitutively expressed in the nucleus of endothelial cells and epithelial cells in vivo: a novel 'alarmin'? *PLoS One* **3**, e3331 (2008).
11. Liew, F. Y., Pitman, N. I. & McInnes, I. B. Disease-associated functions of IL-33: the new kid in the IL-1 family. *Nat. Rev. Immunol.* **10**, 103–110 (2010).
12. Oboki, K., Ohno, T., Kajiwara, N., Saito, H. & Nakae, S. IL-33 and IL-33 receptors in host defense and diseases. *Allergol. Int.* **59**, 143–160 (2010).
13. McHedlidze, T. et al. Interleukin-33-dependent innate lymphoid cells mediate hepatic fibrosis. *Immunity* **39**, 357–371 (2013).
14. Baekkevold, E. S. et al. Molecular characterization of NF-HEV, a nuclear factor preferentially expressed in human high endothelial venules. *Am. J. Pathol.* **163**, 69–79 (2003).
15. Bessa, J. et al. Altered subcellular localization of IL-33 leads to non-resolving lethal inflammation. *J. Autoimmun.* **55**, 33–41 (2014).
16. Zhang, Z. et al. Aspirin inhibits endometrial fibrosis by suppressing the TGF-β1- Smad2 /Smad3 pathway in intrauterine adhesions. *Int. J. Mol. Med.* **45**, 1351–1360 (2020).
17. Ai, Y. et al. lncRNA TUG1 promotes endometrial fibrosis and inflammation by sponging miR-590-5p to regulate Fasl in intrauterine adhesions. *Int. Immunopharmacol.* **86**, 106703 (2020).
18. Bai, X., Liu, J., Cao, S. & Wang, L. Mechanisms of endometrial fibrosis and the potential application of stem cell therapy. *Discov. Med.* **27**, 267–279 (2019).
19. Abudukeyoumu, A., Li, M. Q. & Xie, F. Transforming growth factor-β1 in intrauterine adhesion. *Am. J. Reprod. Immunol.* **84**, e13262 (2020).
20. Gurung, S., Werkmeister, J. A. & Gargett, C. E. Inhibition of transforming growth factor-β receptor signaling promotes culture expansion of undifferentiated human endometrial mesenchymal stem/stromal cells. *Sci. Rep.* **5**, 15042 (2015).
21. Chan, R. W., Schwab, K. E. & Gargett, C. E. Clonogenicity of human endometrial epithelial and stromal cells. *Biol. Reprod.* **70**, 1738–1750 (2004).
22. Chen, K., Zheng, S. & Fang, F. Endometrial stem cells and their applications in intrauterine adhesion. *Cell Transplant*. https://doi.org/10.1177/09636897231159561 (2023).
23. Gargett, C. E., Schwab, K. E. & Deane, J. A. Endometrial stem/progenitor cells: the first 10 years. *Hum. Reprod. Update* **22**, 137–163 (2016).
24. Queckbörner, S. et al. Cellular therapies for the endometrium: an update. *Acta Obstet. Gynecol. Scand.* **98**, 672–677 (2019).
25. Cayrol, C. & Girard, J. P. Interleukin-33 (IL-33): a nuclear cytokine from the IL-1 family. *Immunol. Rev.* **281**, 154–168 (2018).
26. Lefrançais, E. et al. IL-33 is processed into mature bioactive forms by neutrophil elastase and cathepsin G. *Proc. Natl Acad. Sci. USA* **109**, 1673–1678 (2012).
27. Furuyama, K. et al. Continuous cell supply from a Sox9-expressing progenitor zone in adult liver, exocrine pancreas and intestine. *Nat. Genet.* **43**, 34–41 (2011).
28. Valentijn, A. J. et al. SSEA-1 isolates human endometrial basal glandular epithelial cells: phenotypic and functional characterization and implications in the pathogenesis of endometriosis. *Hum. Reprod.* **28**, 2695–2708 (2013).

29. Jeong, J. W. et al. Foxa2 is essential for mouse endometrial gland development and fertility. *Biol. Reprod.* **83**, 396–403 (2010).
30. Li, D. et al. IL-33 promotes ST2-dependent lung fibrosis by the induction of alternatively activated macrophages and innate lymphoid cells in mice. *J. Allergy Clin. Immunol.* **134**, 1422–1432.e11 (2014).
31. Liew, F. Y., Girard, J. P. & Turnquist, H. R. Interleukin-33 in health and disease. *Nat. Rev. Immunol.* **16**, 676–689 (2016).
32. Xu, X. J. et al. The amomum tsao-ko essential oils inhibited inflammation and apoptosis through p38/JNK MAPK signaling pathway and alleviated gentamicin-induced acute kidney injury. *Molecules* **27**, 7121 (2022).

Acknowledgements

We thank Pengfei Zhang for technical assistance as well as Adobe illustrator for creating mouse in Figs. 1–8 graphical. This research was supported by the National Natural Science Foundation of China (No. 82260300), the Central Guiding Local Science and Technology Development Project of Ningxia (No. 2022YDDF0155), and the Ningxia Science and Technology Innovation Leading Talent Project (No. 2022GKLRLX010).

Author contributions

S.L. conceived the study. D.L. and Z.N.Z. participated in the study design and coordination. L.W.Y. performed the animal experiments. F.J.X. performed the Western blotting. Y.L.M. and Y.R.J. performed the pathological experiments. H.X.Z. performed the organoid culture. M.X.C. performed the real-time PCR. S.L. and D.L. drafted the manuscript.

Competing interests

The authors declare no competing interests.

Ethics approval

The study was reviewed and approved by the Ethics Committee of Ningxia Medical University. (1) Title of the approved project: The mechanism by which organoids activate the IL33/st2 pathway to participate in the repair process after endometrial injury. (2) Name of the institutional approval committee: Ethics Committee of Ningxia Medical University. (3) Approval number: KYLL-2022-0460. (4) Date of approval: 17 May 2022.

Additional information

Supplementary information The online version contains supplementary material available at https://doi.org/10.1038/s42003-024-06709-1.

Correspondence and requests for materials should be addressed to Sang Luo.

Peer review information *Communications Biology* thanks the anonymous reviewers for their contribution to the peer review of this work. Primary Handling Editors: Loredana Quadro and Dario Ummarino. A peer review file is available.